13th International Conference on Probabilistic Safety Assessment and Management (PSAM 13)
2~7 October, 2016 • Sheraton Grande Walkerhill • Seoul, Korea • www.psam13.org

ESTIMATING LOSS-OF-COOLANT ACCIDENT (LOCA) FREQUENCIES VIA SPATIO-TEMPORAL METHODOLOGY

Nicholas O'Shea[1], Zahra Mohaghegh[1], Seyed A. Reihani[1], and Ernie Kee[1]

[1] *Department of Nuclear, Plasma, and Radiological Engineering, University of Illinois at Urbana-Champaign, Urbana, Illinois, U.S., 61801, oshea6@illinois.edu, zahra13@illinois.edu, sreihani@illinois.edu, erniekee@illinois.edu*

The South Texas Project Nuclear Operating Company initiated a risk-informed project in 2011 to resolve Generic Safety Issue 191 (GSI-191), which is concerned with pressurized water reactor sump performance for hypothesized loss-of-coolant accident (LOCA) scenarios that result in debris generation. One of the challenges for the GSI-191 project is the estimation of location-specific LOCA frequencies. A LOCA is a critical initiating event in the Probabilistic Risk Assessment (PRA) scenarios for GSI-191. This paper reports on the development of a methodology that explicitly incorporates time and the physical parameters associated with space into the estimations of LOCA frequencies. LOCA frequencies are a function of both underlying degradation mechanisms and repair mechanisms. Therefore, this research uses a Markov modeling technique combined with Probabilistic Physics-of-Failure (PPoF) analysis to develop a spatio-temporal estimation of LOCA frequencies. This spatio-temporal probabilistic methodology can be used to compare the effects that changes in material properties, operating conditions, and maintenance programs have on the probability of LOCA occurrence. This paper presents a case study that compares the time-dependent rupture probabilities due to stress corrosion cracking for the expansion-transition region of steam generator tubes fabricated from Alloy 690 and Stainless Steel.

I. INTRODUCTION

The United States Nuclear Regulatory Commission (NRC) has increased the use of formal risk assessment techniques, such as Probabilistic Risk Assessment (PRA), in order to improve regulatory decision-making.[1-3] The estimation of loss-of-coolant accident (LOCA) frequencies is used in an assortment of risk-informed regulatory applications, including the PRA of nuclear power plants (NPPs). NUREG-1829[4] provides estimations of LOCA frequencies, developed through an expert elicitation process, as a function of component break size for boiling water reactors (BWRs) and pressurized water reactors (PWRs). The experts performing the analysis documented in NUREG-1829 provided "multipliers" for the distributions of LOCA frequencies. These multipliers allow for adjustment from estimates at 25-years of reactor life to 40- or 60-year estimates. Therefore, the temporal effects on LOCA frequencies were *implicitly* considered. These frequencies represent a simple summation of the contributions to LOCA frequencies from all of the locations across the reactor coolant system (RCS). However, the estimations of LOCA frequencies in NUREG-1829 did not *explicitly* provide the contribution to the total LOCA frequencies of each individual location across the RCS. While the experts incorporated their knowledge of the variability of contributions to LOCA frequencies considering their location in the RCS, this knowledge of spatial variation was only *implicitly* incorporated into the final NUREG-1829 results.

For some risk-informed applications, it is important to know how LOCA frequencies vary by RCS location. Generic Safety Issue 191 (GSI-191) is an example of a risk-informed application that requires the estimation of location-specific LOCA frequencies.[5,6] GSI-191 is concerned with PWR sump performance for hypothesized LOCA scenarios that result in debris generation. In 2011, the South Texas Project Nuclear Operating Company (STPNOC) initiated a risk-informed pilot project to resolve GSI-191 by characterizing the risk significance of sump blockage.[7] This project implemented an integrative risk framework (i.e., integration of classical PRA with simulation-based modeling) to provide failure probabilities for the plant-specific PRA basic events associated with GSI-191. The initiating element of this integrated risk framework required the development of location-specific LOCA frequencies. Specifying the locations in the RCS is significant in the GSI-191 project because of the location dependence of the post-LOCA phenomena. For example, two pipes may experience a break of the same size, but the GSI-191 related post-LOCA phenomena (e.g., quantity of debris generation, debris transport fractions, in-vessel flow paths, etc.) may vary significantly depending on the location of the pipe break. Therefore, the STPNOC project needed to develop a method for distributing the cumulative LOCA frequencies, provided in NUREG-1829, to each of the possible break locations in the RCS.

In support of the STPNOC project, Fleming and Lydell[8] distributed the estimations developed in NUREG-1829 across the pipe and nozzle welds of the RCS utilizing surrogate failure data from NPP service experience. Fleming and Lydell

utilized over 4,000 reactor-years of NPP service data to develop surrogate failure rates for each of the major underlying failure mechanisms in a PWR RCS. An event was considered to be a surrogate failure whenever a repair or replacement of a RCS component was required. Each surrogate failure event was attributed to a dominant underlying failure mechanism. These surrogate failures are combined with failure mechanism susceptibility information for each weld in order to determine location-specific surrogate failure rates. The location-specific surrogate failure rates were then combined with conditional rupture probability models derived from information provided in NUREG-1829 in order to develop a location-specific estimation of LOCA frequencies. Fleming and Lydell's study laid the groundwork for the *explicit* inclusion of spatial variation into the estimation of LOCA frequencies. Fleming and Lydell's work *implicitly* considers temporal variation, because it uses the same generic "multipliers" developed by the experts in the NUREG-1829 elicitation. The probability of an RCS component experiencing a rupture changes as components degrade from failure mechanisms. As components degrade, they are more likely to rupture. Thus, as they degrade, components should have an increased contribution to the total LOCA frequencies. Therefore, in order to *explicitly* incorporate temporal variation into the LOCA frequencies, the states of degradation of the components in the RCS need to be considered. Additionally, while NUREG-1829 estimations include non-piping RCS component contributions to LOCA frequencies, Fleming and Lydell's work only includes the contributions from the piping components.

The authors of this paper set out to explore the importance of non-piping components for the estimation of LOCA frequencies in order to determine the significance of the assumption to exclude non-piping components from estimations of LOCA frequencies. The authors conducted evidence-seeking research to more fully understand this significance and concluded that the assumption could not be accepted. The authors determined that a quantitative methodology must be developed in order to properly assess the assumption. Readers may refer to O'Shea et al.[9] for a complete description of the qualitative investigation process as well as examples of both expert analysis and potentially significant non-piping components for the estimation of LOCA frequencies. The spatio-temporal methodology[10] was then developed in order to incorporate the underlying physical failure mechanisms into the estimation of the LOCA frequencies. This methodology provides a quantitative tool, capable of analyzing the contributions of non-piping components to LOCA frequencies, which helps determine the significance of their contributions to the estimations of LOCA frequencies. The spatio-temporal probabilistic methodology is explained in Section II and a case study for the contributions to LOCA frequencies from Stress-Corrosion Cracking (SCC) is provided in Section III.

II. SPATIO-TEMPORAL PROBABILISTIC METHODOLOGY FOR ESTIMATION OF LOCA FREQUENCIES

The underlying mechanisms that affect the state of degradation of a component in the RCS fall into two categories: degradation and repair. In order to capture the back-and-forth nature of the degradation and repair mechanisms, this research uses a Markov modeling approach. Fleming[11] develops a Markov model for piping system reliability that incorporates statistical estimates from Electric Power Research Institute (EPRI) studies performed for thermal fatigue and water hammer events. Fleming's work is an example of a Markov approach based solely on service data. The authors of this paper believe the most accurate modeling approach combines service data with Probabilistic Physics-of-Failure(PPoF) models (i.e., an integration of theory-based and data-oriented approaches), as explained in O'Shea et al.[12] The proposed spatio-temporal probabilistic methodology combines PPoF analysis with Markov modeling based on the following 4 steps:

Step 1: Define Markov States of Degradation; While selecting the states of degradation for the Markov model, the modeler should consider the following three criteria: (1) the desired output information, (2) how state thresholds align with the underlying mechanisms, and (3) the computational cost of the model. Fig. 1 demonstrates a Markov model, developed for the case study in Section III, which depicts the integration of a PPoF causal model for component leakage from SCC. The four ovals on the left side of the figure represent the four Markov states of degradation developed for the case study: New, Flaw, Leak, and Rupture.

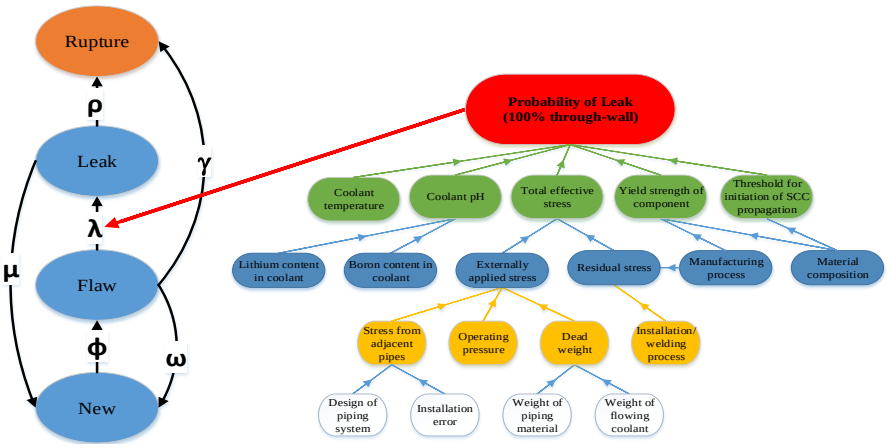

The definitions of each of these states are provided in Section III.

Step 2: Development of Transition Rates; There are two categories of transition rates corresponding to the two categories of underlying mechanisms: degradation and repair. In Fig. 1, the transition rates of degradation are represented by ϕ, λ, ρ, and γ, which represent the pathways of transition from the "New" state to the "Flaw state, "Flaw" to "Leak", "Leak" to "Rupture", and "Flaw" to "Rupture", respectively. The transition rates of degradation provide the *explicit* pathway for connecting the PPoF causal models to the Markov model. In Fig. 1, a SCC causal model is shown on the right-hand side of the image. This causal model can be used to develop the rate at which the probability of a component being in the "Flaw" state will decrease due to transitions into the "Leak" state from SCC. The transition rates are also the *explicit* pathway for incorporation of location-specific factors, since the PPoF causal models change depending on the location of the component. Causal factors such as coolant temperature or material composition are incorporated into the causal models; therefore, the values of the transition rates of degradation change with the values of these parameters. Interested readers may refer to O'Shea at al.[12] for more information regarding the development of Physics-of-Failure (PoF) causal models. Transition rates of repair represent the pathways by which a component can move to a less degraded state. In Fig. 1, the transition rates of repair are represented by ω and μ, which represent the pathways of transition from the "Flaw" state to the "New" state and the "Leak" state to the "New" state, respectively. The transition rates of repair provide the *explicit* pathway for connecting models of maintenance mechanisms.

Step 3: Quantification of Transition Rates; The desired output from a Markov model is a time-dependent distribution of the probabilities that a component resides in each of the states of degradation. There are multiple ways to quantify the transition rates of a Markov model. One method for quantification of transition rates is to use NPP service data, e.g., Fleming,[11] to calculate the occurrence rate of each state. This data-oriented approach enables the modeler to bring historical experience into a Markov model. However, this requires sufficient service data for every possible scenario of concern and also cannot explicitly connect the transition rates to their underlying physical causes. Therefore, incorporation of PPoF models can be a useful way to quantify the transition rates of degradation. Vinod[13] implements a probabilistic approach for quantification of the transition rates of degradation due to erosion corrosion (E-C) for piping components of Pressurized Heavy Water Reactors. This approach incorporates PoF equations for E-C to develop a distribution of the "average" rate of corrosion of a component. Due to this "averaging", Vinod's approach is incapable of explicit incorporation of spatio-temporal effects of physical parameters into the estimation of transition rates. Therefore, an integration of a time-based PPoF approach with a Markov technique is proposed in this paper. In the time based PPoF approach, a PoF causal model for the underlying degradation mechanisms is first developed and the time-to-failure is isolated. Here, time-to-failure does not necessarily mean failure of the component. Time-to-failure could represent the amount of time it takes for a component to reach a specific threshold of degradation (e.g., entering the "Flaw" state). Next, a time-to-failure distribution is developed considering the uncertainties in the input parameters and utilizing a simulation-based modeling. An example of this time-based PPoF approach for quantifying the transition rates of degradation is implemented in the case study (Section III).

Step 4: Developing the Time-Dependent Distribution of State Probabilities; For each state of degradation, a differential equation can represent the rate of change of the probability that a component will be in each state at any given time. Eq. (1-4) are developed for the Markov model shown in Fig.1.

$$\frac{dNew(t)}{dt} = (\omega \cdot Flaw(t)) + (\mu \cdot Leak(t)) - (\phi \cdot New(t)) \quad (1)$$

$$\frac{dFlaw(t)}{dt} = (\phi \cdot New(t)) - (\omega \cdot Flaw(t)) - (\gamma \cdot Flaw(t)) - (\lambda \cdot Flaw(t)) \quad (2)$$

$$\frac{dLeak(t)}{dt} = (\lambda \cdot Flaw(t)) - (\mu \cdot Leak(t)) - (\rho \cdot Leak(t)) \quad (3)$$

$$\frac{dRupture(t)}{dt} = (\rho \cdot Leak(t)) + (\gamma \cdot Flaw(t)) \quad (4)$$

where: New(t), Flaw(t), Leak(t), and Rupture(t) represent the probability that a component will be in each state at a given time, t, and ω, μ, ϕ, γ, λ, and ρ represent the transition rates from Fig. 1. The quantification results for the time-dependent distribution of state probabilities for the case study can be found in Section III.

III. CASE STUDY: ESTIMATION OF LOCA FREQUENCIES IN PWR RCS DUE TO SCC

For this case study, the probabilities of SCC causing a component to reach the rupture state of degradation for components made of Alloy 690 and Stainless Steel (SS) are compared using the spatio-temporal probabilistic methodology introduced in Section II. The final state of the Markov model in this case study is defined as the Rupture state. The

characteristic threshold of the Rupture state is the occurrence of the burst phenomenon, which occurs when the internal pressure of the primary coolant exceeds the capability of the component to withstand the coolant pressure. For the Alloy 690 steam generator tubes, two models are selected for quantifying burst pressures: (1) a model by the American Society of Mechanical Engineers which is a function of axial crack sizes in steam generator tube walls[14] and (2) a model provided in NUREG-6575[15] for a single dominant crack. If the pressure inside a component exceeds the burst pressure of either model, the component is considered to have experienced a burst phenomenon and moves into the Rupture state. The Leak state is the second most-degraded state in the Markov model. For Alloy 690 components, the Leak state is reached when a corrosion crack depth in the component propagates 100% through the thickness of the component wall. Additionally, when the internal pressure of the coolant exceeds the capability of a small "ligament" of remaining component material, a ligament burst phenomenon occurs. A "ligament" of component material occurs when a part-through (not 100% through-wall) crack causes only a small portion of material to remain, which has a reduced capability to withstand the pressure of the internal coolant. Once the internal pressure of the coolant exceeds the capability of the ligament to hold the coolant, the ligament will rapidly fail, forming a 100% through-wall crack. The pressure at which this rapid failure of the ligament occurs is called the ligament pressure. This research selected a model for ligament pressure provided in NUREG-6575.[15] If the internal coolant pressure exceeds the remaining ligament pressure of a component, but does not exceed the burst pressure of the component, the ligament fails rapidly without the component bursting. Therefore, the component will move into the Leak state. A ligament pressure model was not selected for SS components, because the SCC model development for SS in NUREG-6986[16] did not indicate that such behavior also occurred in SS materials. Therefore, SS components only transition into the Leak state when the crack depth propagates 100% through the component wall. The Flaw state is the second least-degraded state in the Markov model developed for this case study. SCC begins propagation in a component once an initial crack is formed from a defect in the component. There are many ways that a defect can form in a material such as from construction deficiencies, external damage, or failure mechanisms. Pitting is often a precursor to SCC due to its combination of local stress concentration and solution chemistry.[17] This research adopts the criterion developed by Kondo,[18] which says that a pit transitions to crack once the SCC growth rate exceeds the pit growth rate, representing a threshold driving force. Therefore, the threshold criteria for the Flaw state are dependent on the selection of both SCC propagation models and pit growth rate models. The least degraded state for this case study is the New state. A component is defined to be in the New state if it does not have any defects that satisfy the threshold criteria to enter into the Flaw state. A component may not be in perfect condition (i.e., have pits or defects), but if none of the pits or defects have become cracks, SCC will not propagate, and the component will be in the New state.

For this case study, General Electric Global Research (GEGR) experimental data[19] for SCC growth rates in Alloy 690 specimens were used to update the SCC propagation model developed by Wu,[20] considering two important changes. The first change was to condense the two-stage model into a one-stage model. Wu wanted to fit a three-stage SCC propagation curve to available experimental data, however, he saw that the third stage occurred very rapidly, so he did not model the third stage. The two-stage model developed by Wu represents the first two stages of the SCC propagation curve. For the first stage, Wu shows that a power law model without a dependency on pH is a sufficient fit for the data. However, for the second stage of Wu's model, the chemical effects were not negligible and pH was needed. When the authors attempted to fit the base SCC model developed by Wu to the GEGR experimental data, it was determined that all dependencies, including chemical dependencies, needed to be incorporated. This determination was made because the authors did not see a transition in the experimental data, such as the one identified by Wu. The second important change to Wu's model was to replace the pH dependency with a Hydrogen content (H_2, cc/kg) dependency. This change was made because quantifying pH at higher temperatures is challenging, since true chemical elements are not known at those temperatures. This means that hydrogen concentrations cannot be easily quantified. Therefore, the authors decided to include hydrogen concentrations directly into the model. The resulting model for Alloy 690 SCC propagation rate (CPR_{690}) is shown in Eq. (5), where: K- stress intensity factor (SIF), T- operating temperature, T_{ref}- reference temperature (588 K), Q- activation energy (130 kJ/mol for Alloy 600), σ_{ys}– material yield strength. One important parameter in the CPR_{690} model is K_{th690}, which represents necessary stress concentration required for SCC to begin propagating in a component fabricated from Alloy 690 material. K_{th600} was developed by Scott[21] for SCC propagation in steam generators made of Alloy 600 material. Scott determined the required stress intensity factor for SCC to propagate in Alloy 600 material to be $9MPa\sqrt{m}$. After analyzing the available experimental SCC data for Alloy 690, the authors determined that the data did not provide sufficient evidence to choose a different value for K_{th690}. Therefore, the authors have selected $K_{th690} = 9MPa\sqrt{m}$.

$$CPR_{690} = C_{690} \cdot \exp\left[\frac{Q}{R}\left(\frac{1}{T} - \frac{1}{T_{ref}}\right)\right] \cdot \left[\sigma_{ys}\right]^{m_{690}} \cdot \left[K - K_{th690}\right]^{n_{690}} \cdot \left[H_2\right]^{\beta_{690}} \qquad (5)$$

For the SS SCC propagation model, the authors utilized experimental data for SCC growth rates in SS developed by Terachi et al.[22] to update the SCC model developed by Wu. After examination of the experimental data, the authors again made an important change to the SCC propagation model developed by Wu. This time, the authors selected a one stage model from Wu's work because no pH dependency could be derived from the available experimental data. The resulting model for SS SCC propagation rate (CPR_{SS}) can be found in Eq. (6). Similar to the case for the CPR_{690} model, the authors needed to determine a value for K_{thSS}. However, for SS the authors decided to select $K_{thSS}=10MPa\sqrt{m}$. The authors determined this value from analysis of the experimental data from Terachi et al[22] and, they believe that the reason for this determination stems from the experimental procedure implemented by Terachi et al., where each specimen was pre-cracked until the stress intensity factor reached $10MPa\sqrt{m}$. Therefore, further research is required to explore the true value of the threshold stress intensity factor for SCC propagation in Stainless Steel materials.

$$CPR_{SS} = C_{SS} \cdot \exp\left[\frac{Q}{R}\left(\frac{1}{T}-\frac{1}{T_{ref}}\right)\right]\cdot\left[\sigma_{ys}\right]^{m_{SS}} \cdot\left[K-K_{thSS}\right]^{n_{SS}} \qquad (6)$$

The empirical model parameters in the Alloy 690 and SS SCC propagation models, C_{690}, m_{690}, n_{690}, β_{690}, C_{SS}, m_{SS}, and n_{SS}, were quantified with Bayesian regression analysis, using OpenBUGS,[23] an open source version of the Bayesian inference Using Gibbs Sampling (BUGS) package. The resulting posterior joint distributions are represented by marginal distributions for each of the model parameters in the SCC propagation model, listed in Table 1.

TABLE 1. SCC Propagation Empirical Model Parameters

Parameter	Mean	Std. Dev.	2.50%	Median	97.50%
C_{690}	3.814E-13	1.000E-10	9.222E-18	9.679E-15	2.972E-12
m_{690}	0.215	0.010	0.005	0.142	0.842
n_{690}	3.220	0.028	2.054	3.212	4.381
β_{690}	0.825	0.598	0.036	0.710	2.092
C_{SS}	9.466E-18	1.000E-10	1.086E-21	2.898E-19	5.505E-17
m_{SS}	2.547	0.441	1.756	2.532	3.430
n_{SS}	1.052	0.434	0.338	0.998	1.989

For this case study, when a component is in the New state, it is assumed that the only mechanism acting upon the component is the mechanism of pitting. This research adopts the pit-to-crack transition criteria developed by Kondo,[18] which considers that a pit will transition into a crack when the SCC propagation rate is greater than or equivalent to the pit growth rate. Therefore, to quantify the transition rate, ϕ, the authors selected a pit growth model developed by Gorman et al.[24] and a Weibull distribution was fit to the experimental data collected for pit growth in de-aerated pure water for 15,402 hours by Turnbull et al.[17] to generate a surrogate initial pit size distribution. Using the developed models for SCC propagation and pit growth, as well as the initial pit distribution, the authors developed a simulation technique that samples from the uncertainty distributions and determines the amount of time required for initial pits to transition into cracks. In order to determine the probability that a pit in the New state will transition to the Flaw state, the number of samples that transition from the New state to the Flaw state is divided by the total number of samples. This fraction provides the probability as the number of samples approaches infinity. The transition rates for a Markov model are rates of probability transition which means the rate at which the probability that a component is in a given state is changing or "flowing" into another state. Therefore, in order to incorporate the rate at which the samples transition from the New state to the Flaw state, the mean time-to-Flaw (MTTF) is calculated. The inverse of the MTTF provides the rate of transition from the New state to the Flaw state. This MTTF only takes into consideration the samples that actually transitioned into the Flaw state within 60 years, so the inverse of the MTTF by itself is insufficient for providing the rate of probability transfer from the New state to the Flaw state. Therefore, the authors multiplied the probability of transition from the New state to the Flaw state by the inverse of the MTTF in order to find the transition rate of probability from the New to the Flaw state. This relationship is represented in Eq. (7).

$$\phi = \left(\frac{\#\,\text{Transitions}\,(New \rightarrow Flaw)}{\text{Total}\,\#\,\text{Samples}}\right) * \left(\frac{1}{MTTF}\right) \qquad (7)$$

The pit growth simulation sampled from model parameters for the SCC propagation rate and pit growth rate as well as the initial pit sizes. Using the Latin Hypercube Sampling approach, the pit growth simulations were run for 400,000 samples for both Alloy 690 and Stainless Steel. The resulting calculations for ϕ are presented in Table 2.

TABLE 2. Calculation of ϕ from Simulation Results of New to Flaw Transitions for Alloy 690 and SS

ϕ	Alloy 690	Stainless Steel
# Samples	400,000	400,000
Fraction of Transitions/Samples	0.99	0.74
MTTT(hours)	11,508	51,910
ϕ(1/hour)	**8.60E-05**	**1.43E-05**

For this work, the SCC propagation models were used to quantify the transition rates λ, γ, and ρ using a time-based probabilistic physics-of-failure approach similar to the one used for the quantification of ϕ. For the initial flaw distribution, a gamma distribution of crack lengths is utilized, which was formulated from 1994 inspection data from a Ringhals Unit 4 steam generator.[25] Using the SCC propagation models developed and the initial flaw length distribution, a simulation is developed to sample from the uncertainty distributions associated with the model parameters and to quantify the transition rates λ, γ, and ρ. The results for the simulations for 400,000 samples are shown in Table 3.

TABLE 3. Calculation of λ, γ, and ρ from SCC Propagation Simulation Results for Alloy 690 and SS

λ	Alloy 690	Stainless Steel
# Samples	400,000	400,000
Fraction of Leaks/Samples	0.507	0.621
MTFF(hours)	31,895	193,439
λ(1/hour)	**1.59E-05**	**3.21E-06**
γ	Alloy 690	Stainless Steel
# Samples	400,000	400,000
Fraction of Ruptures/Samples	0.457	0.100
MTFF(hours)	31,895	193,439
γ (1/hour)	**1.43E-05**	**5.17E-07**
ρ	Alloy 690	Stainless Steel
# Leaks	400,000	400,000
Fraction of Ruptures/Leaks	0.841	0.975
MTLR(hours)	268,886	19,471
ρ(1/hour)	**3.13E-06**	**5.01E-05**

Once a component enters the Flaw or Leak states, there is a possibility that the degradation will be detected and repaired. These repairs could bring a component back into a less-degraded state. In Fig. 1, these possible repair paths are represented by ω and μ. For this case study, the Markov model does not have any repair transition rates from the Rupture state, because it is assumed that once a component ruptures, it cannot be repaired. In order to fix the rupture, the component must be replaced, which would then require the use of a new Markov model for the new component. Additionally, the repair rates from the Flaw and Leak states only transition to the New state, because it is assumed for this case study that all repairs are perfect. For this case study, ω (Flaw to New transition) and μ (Leak to New transition) are quantified using a solely data-informed approach, as was implemented by both Vinod[13] and Fleming.[11] A summary of all of the values for the transition rates of the Markov models developed for this case study can found in Table 4.

TABLE 4. Summary of Values for Transition Rates Used for Quantification of the Markov Models

Transition Rate	690 Value (1/hour)	SS Value (1/hour)
ϕ	8.60E-05	1.43E-05
λ	1.59E-05	3.21E-06
γ	1.43E-05	5.17E-07
ρ	3.13E-06	5.01E-05
ω	2.56E-06	2.56E-06
μ	9.23E-06	9.23E-06

The solutions to Eq. (1-4) for the four Markov states of degradation led to the results summarized in Table 5. The most important result is that the probability of a component made of Stainless Steel will enter the Rupture state increases much more slowly than the probability that a component made of Alloy 690 entering the Rupture state. This is the result that was

expected from the simulations, because Stainless Steel is more resistant to SCC than Alloy 690. The corrosion resistance of each material was captured in the simulation process through the SCC propagation model parameters. It is clear that these parameters have a large effect on the final time-dependent state probability distributions. According to the results of this case study, after 5 years an Alloy 690 fabricated expansion-transition region of a steam generator tube has over a 30% chance to experience a rupture phenomenon. Whereas, for a Stainless Steel fabricated expansion-transition region of a steam generator, the chance is only at 2%. Then after 60 years, the extended lifetime of a NPP, there is a 96% chance of an Alloy 690 component experiencing a rupture, but only a 68% chance of a Stainless Steel component experiencing such a phenomenon. This indicates a very significant effect from material selection on the primary RCS loop. It is important for future work to perform sensitivity analyses on the outputs from the spatio-temporal methodology so that the most important factors can be identified. This identification of the critical factors allows for the most efficient resource allocation for improvement of model accuracy, as well as the improvement of the overall system safety.

TABLE 5. Summary of Time-Dependent State Probability Distribution for Alloy 690 and Stainless Steel

Material	Time (years)	0	1	5	10	20	25	40	60
Alloy 690	N(t)	1.000	0.476	0.057	0.037	0.024	0.018	0.009	0.003
	F(t)	0.000	0.453	0.392	0.176	0.078	0.059	0.027	0.010
	L(t)	0.000	0.036	0.248	0.281	0.185	0.144	0.067	0.024
	R(t)	0.000	0.034	0.303	0.506	0.713	0.778	0.897	0.963
Stainless Steel	N(t)	1.000	0.884	0.558	0.347	0.185	0.152	0.100	0.063
	F(t)	0.000	0.115	0.406	0.547	0.548	0.507	0.374	0.241
	L(t)	0.000	0.001	0.016	0.027	0.030	0.028	0.021	0.014
	R(t)	0.000	0.000	0.020	0.080	0.236	0.313	0.505	0.683

IV. SUMMARY AND CONCLUSION

PRA is an important input to risk-informed regulation for the NRC and the nuclear industry. Estimation of LOCA frequencies is critical for PRA, as LOCAs represent one type of initiating event in the analyses of PRA. However, due to the rare nature of LOCAs, there are insufficient statistical data to develop a purely statistics-based estimation of LOCA frequencies. In 2008, this problem was solved through the implementation of an expert elicitation process, documented in NUREG-1829. The NUREG-1829 estimations implicitly incorporate temporal variation using multipliers developed by experts. The NUREG-1829 estimates do not incorporate explicit spatial variation within the RCS. The GSI-191 related issues date back to 1979. Despite significant efforts by both the NRC and the nuclear industry, GSI-191 could not be resolved using a deterministic approach. In 2011, STPNOC initiated a risk-informed pilot project to resolve GSI-191. One of the critical inputs to the integrative risk framework developed for the project was the estimation of location-specific LOCA frequencies. Since NUREG-1829 estimations were not location-specific, Fleming and Lydell utilized service data to develop a location-specific estimation of LOCA frequencies. Fleming and Lydell's work considered only piping components, since they were thought to be more susceptible to LOCA occurrence. Their work also *implicitly* considered temporal variation of LOCA frequencies. Therefore, this research develops a spatio-temporal methodology to *explicitly* incorporate underlying PoF, specific to each location, at any given time. The methodology is implemented for a SCC case study, summarized in Section III. The explicit incorporation of PPoF has three main benefits: (1) the estimation of LOCA frequency is more accurate because of the explicit incorporation of operating conditions and maintenance quality, (2) tt allows for a more accurate prevention strategy, since the root causes of LOCA can be identified and ranked through sensitivity analysis. This allows for more efficient allocation of resources to increase safety, as well as to increase profit from more efficient maintenance strategies, and (3) it facilitates integration of PPoF-based LOCA initiating events to PRA, which allows for the ranking of the most important contributors for risk. This benefits risk-informed regulation for nuclear power plants.

ACKNOWLEDGMENTS

This material is based upon work supported under an Integrated University Program Graduate Fellowship. The authors thank the South Texas Nuclear Operating Company for providing information for this project. Thanks also to all members of the Socio-Technical Risk Analysis (SoTeRiA) Laboratory in the Department of Nuclear, Plasma, and Radiological Engineering for their feedback, especially, undergraduate intern, Ethan Graven, for his support with the computational runs.

REFERENCES

1. U.S. Nuclear Regulatory Commission, *An Approach for Using Probabilistic Risk Assessment in Risk-Informed Decisions on Plant-Specific Changes to the Licensing Basis,* U.S. NUCLEAR REGULATORY COMMISSION, Regulatory Guide 1.174 (1998).
2. G. APOSTOLAKIS, "*A Proposed Risk Management Regulatory Framework*," United States Nuclear Regulatory Commission, Risk Management Task Force (2012).
3. U. S. Nuclear Regulatory Commission, *Use of Probabilistic Risk Assessment Methods in Nuclear Regulatory Activities; Final Policy Statement*, A. BATES, 60, 158, Federal Register, p. 42622 (1995).
4. R. TREGONING et al., "*Estimating Loss-of-Coolant Accident (Loca) Frequencies through the Elicitation Process*," United States Nuclear Regulatory Commission, NUREG-1829 (2008).
5. B. A. BOGER, "*Potential Impact of Debris Blockage on Emergency Recirculation During Design Basis Accidents at Pressurized-Water Reactors*," NRC Generic Letter 2004-02, United States Nuclear Regulatory Commission Office of Nuclear Reactor Regulation, ML042360586 (2004).
6. M. R. FARD, "*Issue 191: Assessment of Debris Accumulation of Pwr Sump Performance*," Division of Risk Analysis, NUREG-0933 Resolution of Generic Safety Issues, 2 (2011).
7. Z. MOHAGHEGH et al., "Risk-Informed Resolution of Generic Safety Issue 191,*" Proceedings of the International Topical Meeting on Probabilistic Safety Assessment and Analysis,* LaGrange Park, IL, USA, American Nuclear Society (2013).
8. K. FLEMING et al., "*Development of Loca Initiating Event Frequencies for South Texas Project Gsi-191*," South Texas Project Nuclear Operating Company, Revision 1 (2011).
9. N. O'SHEA et al., "Analyzing Non-Piping Location-Specifc Loca Frequency for Risk-Informed Resolution of Generic Safety Issue 191,*" Proceedings of the International Topical Meeting on Probabilistic Safety Assessment and Analysis,* Sun Valley, ID, USA, p. 499, American Nuclear Society (2015).
10. N. O'SHEA and Z. MOHAGHEGH, "Spatio-Temporal Methodology for Estimating Loss-of-Coolant Accident Frequencies in the Risk-Informed Resolution of Generic Safety Issue 191,*" Proceedings of the American Nuclear Society Student Conference,* (2016).
11. K. N. FLEMING, "Markov Models for Evaluating Risk-Informed in-Service Inspection Strategies for Nuclear Power Plant Piping Systems,*" Reliability Engineering & System Safety,* **83,** *1*, 27 (2004).
12. N. O'SHEA et al., "Physics of Failure, Predictive Modeling and Data Analytics for Loca Frequency,*" Proceedings of the Annual Reliability & Maintainability Symposium (RAMS),* IEEE (2015).
13. G. VINOD et al., "A Comprehensive Framework for Evaluation of Piping Reliability Due to Erosion–Corrosion for Risk-Informed Inservice Inspection,*" Reliability Engineering & System Safety,* **82,** *2*, 187 (2003).
14. P. MACDONALD et al., "*Steam Generator Tube Failures*," Idaho National Engineering Laboratory, NUREG/CR-6365 (1996).
15. S. MAJUMDAR et al., "*Failure Behavior of Internally Pressurized Flawed and Unflawed Steam Generator Tubing at High Temperatures - Experiments and Comparison with Model Predictions*," Argonne National Laboratory, Washington D.C., USA, NUREG/CR-6575 (1998).
16. M. KHALEEL and F. SIMONEN, "*Evaluations of Structural Failure Probabilities and Candidate Inservice Inspection Programs*," Pacific Northwest National Laboratory, NUREG/CR-6986 (2009).
17. A. TURNBULL et al., "A Model to Predict the Evolution of Pitting Corrosion and the Pit-to-Crack Transition Incoporating Statistically Distributed Input Parameters,*" Corrosion Science,* **48**, 2084 (2006).
18. Y. KONDO, "Prediction of Fatigue Crack Initiation Life Based on Pit Growth,*" Corrosion Science,* **45,** *1*, 7 (1989).
19. ELECTRIC POWER RESEARCH INSTITUTE, "*Materials Reliability Program: Resitance of Alloys 690, 152, and 52 to Primary Water Stress Corrosion Cracking* " Report No 3002000190, J. Hickling, Technical Update, April 2013, Palo Alto, CA, USA, MRP-237, Rev. 2, Appendix L (2013).
20. G. WU, "*A Probabilistic-Mechanistic Approach to Modeling Stress Corrosion Cracking Propagation in Alloy 600 Components with Applications*," Master of Science Thesis, University of Maryland, College Park (2011).
21. P. SCOTT, in *NEA/CSNI - UNIPEDE Specialist Meeting on Operating Experience with Steam Generators* (Framatome, 1991).
22. T. TERACHI et al., "Scc Growth Behaviors of Austenitic Stainless Steels in Simulated Pwr Primary Water,*" Journal of Nuclear Materials,* **426**, 59 (2012).
23. N. THOMAS, Overview of Bugs, http://www.openbugs.net/w/FrontPage (2009).
24. J. GORMAN et al., "Prediction of the Performance of Tubes in Steam Generators in Pressurized Water Reactors,*" Proceedings of the Life Prediction of Corrodible Structures,* NACE (1991).
25. J. GORMAN et al., "*Estimating Probable Flaw Distributions in Pwr Steam Generator Tubes (Nureg/Cr-6521),*" Nuclear Regulatory Commission/ Argonne National Laboratory, Washington D.C., USA (1998).